Does Cytolysis by CD8$^+$ T Cells Drive Immune Escape in HIV Infection?

Mehala Balamurali,* Janka Petravic,* Liyen Loh,† Sheilajen Alcantara,† Stephen J. Kent,† and Miles P. Davenport*

CD8$^+$ "cytotoxic" T cells are important for the immune control of HIV and the closely related simian models SIV and chimeric simian–human immunodeficiency virus (SHIV), although the mechanisms of this control are unclear. One effect of CD8$^+$ T cell-mediated recognition of virus-infected cells is the rapid selection of escape mutant (EM) virus that is not recognized. To investigate the mechanisms of virus-specific CD8$^+$ T cell control during immune escape in vivo, we used a real-time PCR assay to study the dynamics of immune escape in early SHIV infection of pigtail macaques. For immune escape mediated by cytolysis, we would expect that the death rate of wild type (WT) infected cells should be faster than that of EM-infected cells. In addition, escape should be fastest during periods when the total viral load is declining. However, we find that there is no significant difference in the rate of decay of WT virus compared with EM virus. Further, immune escape is often fastest during periods of viral growth, rather than viral decline. These dynamics are consistent with an epitope-specific, MHC class I-restricted, noncytolytic mechanism of CD8$^+$ T cell control of SHIV that specifically inhibits the growth of WT virus in vivo. ***The Journal of Immunology*****, 2010, 185: 5093–5101.**

CD8$^+$ T cell-mediated immune responses are thought to be important for the control of acute and chronic viral growth in HIV and SIV infections. This is supported by several lines of evidence: 1) CD8$^+$ lymphocyte depletion leads to increased viral replication and accelerated disease progression in SIV-infected rhesus macaques (1, 2), 2) CD8$^+$ T cell expansion coincides with the decrease in viral load in the acute phase of infection (3), 3) immune pressure exerted by CD8$^+$ T cells often results in viral escape mutations (4–6), and 4) expression of certain HLA class I alleles is strongly associated with durable disease control (7–9). Taken together, this provides strong evidence that CD8$^+$ T cells play a role in viral control, and that CD8$^+$ T cell pressure causes escape.

Despite strong evidence for the role of CD8$^+$ T cells in controlling HIV viremia and disease progression, the cellular and molecular mechanisms of this control in vivo are unclear. The proposition that viral control is mediated by CD8$^+$ T cell lysis of infected cells is supported by in vitro studies, showing that CD8$^+$ T cells are able to recognize and lyse cells bearing viral-derived peptides bound to host MHC (10, 11). Similarly, in vivo studies have demonstrated clearance of SIV peptide-pulsed cells in infected animals (12). However, the proposed cytolytic mechanism of viral control has been challenged by several studies using CD8$^+$ lymphocyte depletion of SIV-infected macaques to analyze the viral dynamics in SIV in vivo (2, 13, 14). The recent studies of the decay of virus under therapy in the presence and absence of CD8$^+$ T cells have suggested that CD8$^+$ T cells do not alter the rate of decay of productively infected cells (13, 14). These studies of the effects of CD8$^+$ T cell depletion are complicated by both the potential nonspecific effects of the Ab (which also depletes NK cells, for example) and the immune-activating effects of T cell depletion (15). Although recent studies have suggested that immune activation is neither necessary nor sufficient to produce the viral load increases seen after CD8$^+$ T cell depletion during acute SIV infection (15), the problem of a generalized effect on immune function after CD8$^+$ T cell depletion cannot be eliminated.

An alternative to these studies of the effects of CD8$^+$ T cell depletion is to study the effects of enhanced CD8$^+$ T cell targeting of the viral epitopes after vaccination. Successful vaccination can increase the number of virus-specific CD8$^+$ T cells at the peak of infection ~10-fold compared with unvaccinated animals. This, in turn, is associated with a >10-fold reduction in peak viral load in vaccinated animals compared with control animals (16, 17). If this control of infection were mediated by killing of infected cells, then this should result in a large reduction in infected cell life span and correspondingly more rapid decay in virus after the peak of infection (18). However, the rate of decline of viral loads after the peak of infection is not more rapid in vaccinated than unvaccinated animals, and does not correlate with either CD8$^+$ T cell numbers or the level of viral control (19, 20). Thus, it is difficult to understand how vaccine-induced, virus-specific CD8$^+$ T cells could reduce peak viral loads 10-fold through the killing of infected cells without reducing the life span of infected cells (18). One major caveat to these studies is that viral control was observed in different animals, where the levels of virus-specific Abs and CD4$^+$ T cells may also vary. This highlights the need for direct studies of viral dynamics in situations where the only difference in virus environment is in the level of recognition by CD8$^+$ T cells.

Early HIV and SIV infection are frequently characterized by the rapid mutation of virus and the selection of "immune escape variants" that evade CD8$^+$ T cell recognition. We have previously characterized an immunodominant CD8$^+$ T cell epitope in Gag

*Complex Systems in Biology Group, Centre for Vascular Research, University of New South Wales, Sydney, New South Wales; and †Department of Microbiology and Immunology, University of Melbourne, Melbourne, Victoria, Australia

Received for publication July 1, 2010. Accepted for publication August 19, 2010.

This work was supported by the National Health and Medical Research Council and the Australian Research Council.

Address correspondence and reprint requests to Prof. Miles P. Davenport, Centre for Vascular Research, School of Medical Sciences, Faculty of Medicine, University of New South Wales, Sydney, New South Wales, 2052, Australia. E-mail address: m.davenport@unsw.edu.au

Abbreviations used in this paper: EM, escape mutant; QRT-PCR, quantitative real-time PCR; SHIV, simian–human immunodeficiency virus; WT, wild type.

Copyright © 2010 by The American Association of Immunologists, Inc. 0022-1767/10/$16.00

(KP9) restricted through the *Mane-A*10* allele that escapes soon postinfection. We have also developed a real-time PCR assay to measure the levels of WT and escape mutant (EM) virus in vivo. This assay allows us to measure ratios of WT and EM virus down to as low as 1 in 10^4 copies. By measuring the frequency of each viral variant at the KP9 epitope over time, we can now analyze the rate of selection of the unrecognized EM virus compared with the recognized wild type (WT) virus during acute infection. Importantly, this provides an opportunity to study the effects of differential $CD8^+$ T cell recognition on viral dynamics in a natural setting without $CD8^+$ lymphocyte depletion. That is, we have two viral variants that differ in their recognition by KP9-specific T cells but are otherwise exposed to the same host environment. Cells infected with either variant are subject to killing because of other factors such as viral cytopathic effect, Ab-dependent cell-mediated cytotoxicity, NK cell killing, or the effects of T cells recognizing other epitopes. However, only the WT variant is subject to inhibition by KP9-specific CD8 T cells, causing the rapid replacement of the recognized (WT) variant by the unrecognized EM virus in the first weeks of infection. By observing the rate of replacement of WT virus by EM virus, we can measure the rate of immune escape, and thus quantify the additional immune pressure KP9-specific $CD8^+$ T cells exert on the WT virus (compared with the unrecognized EM virus). If escape is driven by cytolysis, then the rate of immune escape should correspond to the increased rate at which cells infected with WT virus are killed relative to EM-infected cells. In contrast, escape could be driven by noncytolytic effects of KP9-specific CD8 T cells, which selectively inhibit the growth of WT virus. For example, KP9-specific T cells may act to reduce viral production by WT-infected cells. In this case, noncytolytic control should lead to WT and EM virus having similar decay rates, because they are affected equally by viral cytopathic effects and other (non–KP9-mediated) immune responses. We show that analysis of the in vivo viral dynamics during acute simian–human immunodeficiency virus (SHIV) infection supports a noncytolytic mechanism of immune control by $CD8^+$ T cells in vivo.

Materials and Methods

Animals and infection

Escape kinetics were studied in 11 *Mane-A*10*$^+$ pigtail macaques (*Macaca nemestrina*) studied as part of a previously reported SHIV vaccine experiment (21). They were infected with $SHIV_{mn229}$ stock (CXCR4-tropic virus containing 10% WT and 90% K165R SIV Gag mutation [EM]). When these animals are infected with SHIV, the immunodominant epitope recognized by $CD8^+$ T cells is the *Mane-A*10* restricted Gag epitope $KP9_{164–172}$ (22). The high $CD8^+$ T cell pressure causes rapid selection of EM virus at the KP9 epitope. The K165R mutation at KP9 dominates the viral quasispecies because it affects the MHC anchor residues (22) and leads to loss of KP9-specific $CD8^+$ T cell recognition. Seven macaques had received T cell–based vaccines (animals 5616, 6276, 6279, and 6370, DNA prime and fowlpox virus boost vaccines; animal 6349, vaccinia prime and fowlpox virus boost vaccine; 5614 and 6351, DNA vaccines only) before the $SHIV_{mn229}$ challenge, whereas animals 5619, 5712, 6167, and 6352 served as unvaccinated control animals.

Virology and immunology studies

The dynamics of EM and WT virus at the SIV Gag KP9 epitope was measured using a quantitative real-time PCR (QRT-PCR) assay described previously (23). In brief, the assay uses a forward primer specific for either the WT sequence or the nucleotide mutation encoding the dominant K165R KP9 EM. At each time point postinfection, 10 μl plasma RNA was reverse-transcribed and then amplified by QRT-PCR using either WT or EM forward primers. A common reverse primer and FAM-labeled DNA probe were also added for quantification against the appropriate SIV Gag epitope RNA standards using an Eppendorf Realplex^4 cycler (Eppendorf, Hamburg, Germany). Analysis was performed using Eppendorf Realplex software. Baselines were set two cycles earlier than real reported fluorescence, and threshold value was determined by setting threshold bar within the linear data phase. Samples amplifying after 40 cycles were regarded as negative and corresponded to <1.5 $\log_{10}$ SIV RNA copies/ml plasma. One of the problems associated with the measurements of escape rates is the frequency of sampling, especially during the acute phase when viral load changes rapidly. This problem is much more severe in the escape studies in HIV, where the range in sampling periods is between 2 wk and several months (24, 25). In our study, animals were sampled every 3–7 d up to day 28, allowing close analysis of viral dynamics. In addition, the QRT-PCR assay permits a large dynamic range over which viral loads can be assessed (allowing measurement of fractions as low as 10^{-4}). This combination of frequent sampling and detecting of low levels of virus allows more accurate measurement of escape rates. However, we note that because the fitness cost in our infection model is small relative to the escape rate (22), it may not always be possible to measure the impact of fitness cost on escape rate.

KP9-specific $CD8^+$ T cell responses were studied on serial blood samples using a Mane-A*10/KP9 tetramer and flow cytometry as previously described (26). CD4 T cell depletion in peripheral blood was analyzed by flow cytometry as previously described (27).

Estimating escape rate from experimental data

The experimental data typically contain viral loads for WT (W) and EM (M) at different time points. The growth rates of WT and EM, g_W and g_M, respectively, are defined between end points of a time interval. If viral loads are measured at time points t_s and t_e, the growth rates of WT g_W and EM g_M in a time interval starting at t_s and ending at t_e are determined from the experimental data as follows:

$$g_W(t_s,t_e)=\frac{\ln[W(t_e)/W(t_s)]}{t_e-t_s}$$
$$g_M(t_s,t_e)=\frac{\ln[M(t_e)/M(t_s)]}{t_e-t_s}. \quad (1)$$

The growth rate is the average rate of exponential growth between the end points of the time interval. Negative growth rate implies decay. In the time interval between t_s and t_e, escape rate is defined (22, 28) as the difference between growth rates of EM and WT in the same interval,

$$E(t_s,t_e)=g_M(t_s,t_e)-g_W(t_s,t_e)=-\frac{\ln[z(t_e)/z(t_s)]}{t_e-t_s}, \quad (2)$$

where $z(t) = W(t)/M(t)$. The escape rate represents the net effect of the WT-specific $CD8^+$ antiviral effect on the virus (A_w), as well as the relative growth of the two strains. We have previously shown that the WT virus has a significant growth advantage over EM virus in the absence of WT-specific $CD8^+$ T cell recognition (the "fitness cost" of escape) (22, 28). The EM virus must first overcome this replicative disadvantage before it can benefit from the $CD8^+$ antiviral effects. Thus, if we know the difference between WT and EM replicative capacities in the absence of $CD8^+$ T cell effects ($r_{W0} - r_M$), and the measured escape rate (E), we can calculate the magnitude of the WT-specific antiviral effect (A_W) in the time interval (t_s, t_e) as (28)

$$A_W(t_s,t_e)=E(t_s,t_e)+(r_{W0}-r_M)T(t_s,t_e), \quad (3)$$

where $T(t_s, t_e)$ is the average number of $CD4^+$ T cells in the interval, and $r_{W0} - r_M$ is the replicative advantage of WT virus without immune selection at the mutant epitope. We have found previously that $(r_{W0} - r_M)T_0$, where T_0 is the baseline plasma $CD4^+$ T cell count, does not differ much between the animals infected by $SHIV_{mn229}$, and is, on average, equal to 0.387/d. We used this value to estimate the second term on the right-hand side in Equation 3. The method of estimating the WT-specific antiviral effect is described in detail by Petravic and colleagues (28).

Modeling the dynamics of viral escape

The simplest model of escape is based on the standard model of virus dynamics (29, 30), with WT (W) and EM (M) competing for infection of target cells,

$$\frac{dI_W}{dt}=k_W WT-\delta_W I_W$$
$$\frac{dI_M}{dt}=k_M MT-\delta_M I_M$$
$$\frac{dW}{dt}=p_W I_W-cW$$
$$\frac{dM}{dt}=p_M I_M-cM. \quad (4)$$

In Equation 4, T is the time-dependent number of uninfected $CD4^+$ T cells that are targets for infection by the virus, and represents the

common environment in which both strains grow. In this infection, we used a CXCR4-tropic virus, which targets both naive and memory $CD4^+$ T cells, so that the $CD4^+$ T cell number in blood is a good measure of available target cells.

I_W and I_M are the cells infected by WT and EM, respectively. The infectivities k_W and k_M characterize the rate of infection of target cells by WT or EM, and δ_W and δ_M are the death rates of cells infected by WT or EM, respectively. Production rates of free WT and EM virus are p_W and p_M, whereas we assume that the free virus clearance rate, c, does not depend on viral strain. This model implies not only a simple dynamics of target cells, infected cells, and virus, but also neglects the possibility of the properties of WT and EM virus changing in time because of compensatory mutations. We have also neglected the mutation of EM into WT and vice versa during the course of infection.

Because the turnover of virions is generally faster than the turnover of infected cells ($c >> \delta_i$, where $i = W,M$), the number of infected cells closely follows the viral load, $I_W = (c/p_W)W$ and $I_M = (c/p_M)M$, so that the instantaneous rates of exponential growth g_W and g_M of WT and EM can be to a good approximation written as (31)

$$g_W = r_W(t)T(t) - \delta_W(t)$$
$$g_M = r_M(t)T(t) - \delta_M(t), \quad (5)$$

where $r_W = k_W p_W/c$ and $r_M = k_M p_M/c$ are the (generally time-dependent) replicative capacities of WT and EM, respectively. Replicative capacity is a compound effect of virus infectivity and production. Viral replication rate denotes the product of the replicative capacity (which is intrinsic to the viral strain) and the target cell number ($r_W T$ and $r_M T$ are the replication rates of WT and EM, respectively); this should be differentiated from the growth rates g_W and g_M. An escape mutation generally carries a "fitness cost," so that the replicative capacity of EM, r_M, is inherently lower than the replicative capacity of WT, r_W. Fitness cost of mutation is the difference in replication rates of WT and EM, $(r_W - r_M)T$, so that it has the strongest effect when target cells are at their highest level. Viral growth rate is the balance of replication and death. Positive values of g_W and g_M, when replication exceeds death, imply an increase in viral load of each type, whereas negative values imply decay.

We define the instantaneous escape rate $E(t)$ at a given time t as the difference of growth rates of EM and WT (EM growing faster because of the selective immune pressure of WT),

$$E(t) = g_M - g_W \equiv \delta_W - \delta_M - (r_W - r_M)T. \quad (6)$$

We assume that WT and EM sequences differ only in one epitope, and that the mutant epitope is not recognized by the KP9-specific response. Both WT- and EM-infected cells may be killed by viral cytopathic effect or immune-mediated killing through other epitopes, which might be thought of as the background death rate of infected cells.

If the $CD8^+$ T cell antiviral effect at the WT epitope is mainly cytolytic, escape occurs when preferential killing of WT-infected cells overcomes its replicative advantage. The difference in death rates, $\delta_W - \delta_M$, represents the rate at which WT-infected cells are preferentially killed. However, if we allow the possibility of cytokine-mediated suppression of viral replication being epitope-specific, then a pure WT-specific noncytolytic effector function would cause escape by preferentially lowering the replicative capacity of WT from its initial value (r_{W0}, where $r_{W0} > r_M$) to a new value in the presence of $CD8^+$ antiviral effect (r_W, where $r_W < r_M$) (whereas leaving the death rates of infected cells the same).

If we know the inherent difference in replicative capacities of WT and EM (without WT-specific immune response) $r_{W0} - r_M$, we can define the WT-specific antiviral effect A_W as (28)

$$A_W = E(t) + (r_{W0} - r_M)T. \quad (7)$$

The first term on the right-hand side is escape rate—that is, the difference between the growth rates of EM and WT in the presence of WT-specific immune pressure. The second term is the difference in the WT and EM growth rates in the absence of WT-specific response (because of the fitness cost of escape). Altogether, the WT-specific antiviral effect measures the specific immune pressure exerted on the KP9 epitope. If the WT inhibition is purely cytolytic, then the WT antiviral effect is, in fact, the killing rate at the WT epitope ($=\delta_W - \delta_M$), corrected for the initial growth advantage of the WT virus, at the number of remaining target cells to infect ($(r_{W0} - r_W)T$). However, if we assume that the $CD8^+$ T cell antiviral effect is epitope-specific, but mediates noncytolytic suppression of viral replication, then the death rates of WT and EM virus are the same. In this case, the antiviral effect is due to the decrease in WT replicative capacity ($A_W = (r_{W0} - r_W)T$), and thus scales with target cell number.

In the case of pure cytolysis ($\delta_W > \delta_M$; $r_W > r_M$), Equation 6 implies that the maximum escape rate is at the lowest $CD4^+$ T cell count, $T_{\min}$. The lowest $CD4^+$ T cell level marks the maximum decay rate of total viral load, $V = W + M$. Therefore, the fastest immune escape rate should be during viral decay after the peak viral load. Similarly, in an earlier study of escape dynamics in SIV (25), it was pointed out that maximum escape caused by cytolysis should be expected during the period of "reduced viral replication," that is, during viral decay.

This expectation relies on the assumption that, in the absence of WT-specific immune pressure, fitness cost of escape mutation will be directly proportional to $CD4^+$ T cell number. We have studied reversion of the same virus to WT in *Mane-A*10*$^-$ animals, where the reversion rate is equivalent to the fitness cost of mutation (or the difference in replication rates of the two viral strains). We have shown that reversion rate is indeed directly proportional to $CD4^+$ T cell numbers measured in blood (28).

Maximum escape rate of a viral variant should not be confused with the maximum probability of a mutation surviving and growing, which is during high viral replication in the context of incomplete immunologic pressure (28, 32). Because in $SHIV_{mn229}$ the mutation is already present in the inoculum, this eliminates the effects associated with the probability and time of appearance of mutation. The change of the WT/EM ratio is then governed by the interplay of immune pressure and availability of the $CD4^+$ T cells.

In the interval of the highest escape rate (when $T = T_{\min}$), the first term on the right-hand side of Equation 5 for viral load slope is at its minimum, so that the decay rate of a viral strain after the peak follows the death rate of infected cells to a good approximation. Consequently, we expect the decay rate of EM to be noticeably lower than the decay rate of WT when immune response is purely cytolytic.

In the case when the SHIV-specific $CD8^+$ T cell response is purely noncytolytic ($\delta_W = \delta_M$; $r_W < r_M$; $E = (r_W - r_M)T$), maximum escape happens at high target cell count, so that the maximum escape rate should be during viral growth. In addition, the decay of WT after the peak should be similar to decay of EM.

Results

WT virus does not decay more rapidly than EM virus

Infection of macaques with SHIV leads to the rapid growth of virus, followed by a peak and decline of virus approximately after day 14. We have previously determined that the $SHIV_{mn229}$ challenge stock contains a mix of 10% WT and 90% EM virus at the KP9 epitope, and studied that rate of immune escape and reversion in $SHIV_{mn229}$-infected animals and the impact of vaccination (22, 23, 32). In this work, we analyzed *Mane-A*10*$^+$ pigtail macaque animals included within a previously reported SHIV vaccine study (21). The rate of immune escape is a measure of how rapidly the proportion of EM virus increases relative to WT virus (irrespective of total viral loads). We also measured the absolute growth rate of total virus or the WT and EM strains simply by measuring the rate at which the strain grows or decays between two sampling times.

Consistent with our previous studies, the average rate of decay of total virus from its peak was $0.69 \pm 0.08\ d^{-1}$, equating to a half-life of 1.0 d. Immune escape is measured by comparing the levels of WT and EM viruses using an real-time PCR assay (Fig. 1). Immune escape was observed in all animals, and the maximum rate of escape was similar to that previously reported ($0.73\ d^{-1}$) (22). The simplest mechanism that can explain rapid immune escape is the selective killing of cells infected with WT virus by KP9-specific cells, leading to the selection of cells infected with EM virus. Therefore, we studied the dynamics of WT and EM virus in blood during acute infection to understand whether selective killing of WT-infected cells was compatible with the observed kinetics.

If immune escape is driven by KP9-specific $CD8^+$ T cell cytolysis of WT-infected cells, one would expect that the WT-infected cells (and virus) should decay faster than the EM virus, because of killing by KP9-specific cells. That is, under a cytolytic assumption, the escape rate is driven only by differences in the

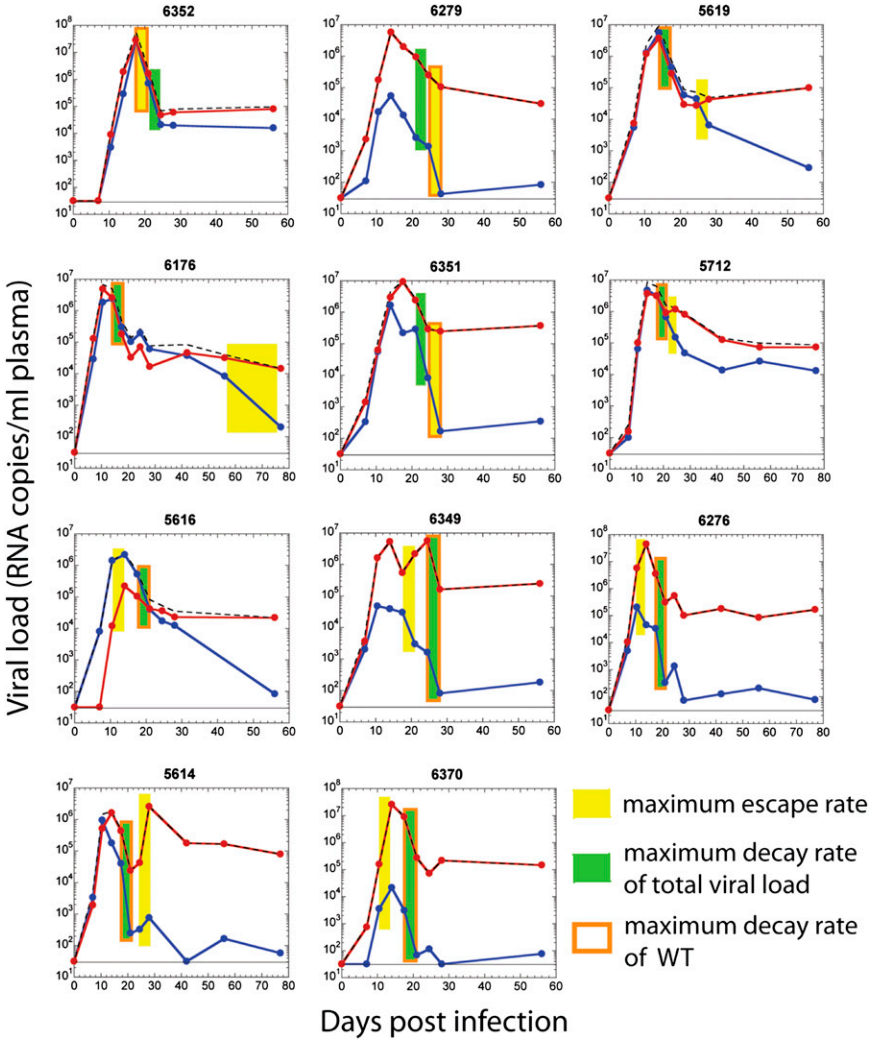

FIGURE 1. Pattern of escape at KP9 epitope in vivo. The levels of wild type (WT; blue) and escape mutant (EM) virus (red) are shown for 11 macaques. The maximum escape rate (yellow rectangles), the maximum decay rate of WT virus (orange rectangles), and the maximum decay of total viral load (green rectangles) are shown. In only 3 in 11 cases does the maximal escape rate coincide with the maximal decay rate of WT virus. In many animals, maximum escape rate occurs during a period of growth in total viral load. Animals are arranged according to the total viral growth rate at which we observe maximum escape rate, ranging from negative (decay) to positive (growth).

death rate of WT- and EM-infected cells. Thus, we would expect WT death rate to be equal to the EM death rate plus the escape rate. When the rate of escape is 0.73 d^{-1}, we might expect that the decay rate of WT virus should be approximately equal to 1.43 d^{-1}, which is the sum of the escape rate (0.73 d^{-1}) and the EM decay rate (e.g., 0.71 d^{-1}).

However, when we compared the maximum rates of decay of WT and EM virus during acute infection, we found they were not significantly different (Fig. 2*A*). Although there was considerable variation in the measured decay rates between animals, the trend was toward a greater decay rate of EM virus, rather than faster decay of WT virus (median decay rate of EM virus was 0.71 d^{-1}, and of WT virus was 0.59 d^{-1}; $p = 0.0534$). Thus, the differences in death rates do not combine to produce the observed decay rate and do not fit a conceptual model where $CD8^+$ T cell activity shortens the life span of cells infected with WT virus. A noncytolytic mechanism of immune escape would imply that WT- and EM-infected cells die at the same rate, but that $CD8^+$ T cells mediate viral control by reducing the infection rate of new cells or reducing viral production from infected cells, and that they would do so preferentially for WT as compared with EM viruses. In either case, we would predict that the decay rates of WT and EM cells should be the same, consistent with our experimental data.

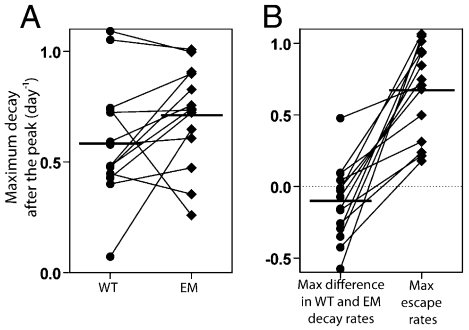

FIGURE 2. Rate of decay of wild type (WT) and escape mutant (EM) virus is not significantly different. *A*, Maximum decay rates of WT and EM virus are not significantly different. *B*, The difference in decay rate between WT and EM does not explain the rate of immune escape in SHIV. Horizontal lines represent the median values.

Similarly, if escape rate were driven by a difference in the death rates of WT- and EM-infected cells, then we might expect that the difference in maximum WT and EM decay rates should determine the maximum rate of escape. However, if we compare the maximum escape rate with the difference between maximum WT and maximum EM decay, we find that differences in decay cannot account for the rate of immune escape (Fig. 2*B*). Indeed, the observed maximum escape rate (0.73 d^{-1}) was faster than the decay rate of either WT or EM virus.

Finally, if immune escape is driven by preferential killing of WT-infected cells, then we would expect that the maximum escape

rate should coincide in time with the maximum decay rate of WT-infected cells. However, despite analyzing samples closely spaced over time (every 2–5 d during the first 4 wk), only in 3 of 11 animals does maximum escape coincide with maximum WT decay (where orange and yellow rectangles coincide in Fig. 1). Indeed, almost half of the animals have maximal immune escape during periods of viral growth (5616–6370 in Fig. 1 are all during total viral growth).

The fastest immune escape occurs during periods of high viral growth

The absence of any difference in the maximum decay rates of WT and EM virus prompted us to examine the speed and timing of immune escape in our cohort (Fig. 1), and to apply a mathematical modeling approach to understanding these dynamics. The dynamics and timing of immune escape were highly variable between animals. In four animals (Fig. 1, animals 6352, 6279, 6176, and 6351), the maximum rate of immune escape occurred during periods when both viruses were decaying, and the WT virus was decaying more quickly than the EM virus. Interestingly, in some of these cases (see, for example, animals 6279 and 6176 in Fig. 1), although EM was decaying more slowly than WT during this period, the maximum decay rate of EM occurred at another time and was similar to the maximum decay rate of WT virus. Only in 1 of 11 cases did the maximum WT decay rate appear substantially faster than the maximum EM decay rate (animal 5616).

If escape is driven by cytolysis, we expect that the maximum escape will occur when the effects of killing WT-infected cells are strongest (i.e., when the decay of total viral load is fastest). However, the maximum escape coincided with maximal viral load decay in only 2 of 11 animals. By contrast, if escape is driven by noncytolytic mechanisms limiting WT viral growth, then we expect to see the fastest escape during periods of viral growth. Consistent with the noncytolytic mechanism, in a number of animals, the most rapid immune escape occurred during periods when either both EM and WT viruses were growing (but EM growing faster than WT; 2/11 animals) or total viral load (and EM virus) was growing and WT virus decaying (3/11 animals). To better understand these dynamics, we modeled the effects of cytolytic and noncytolytic control of virus by $CD8^+$ T cells, and the impact on viral dynamics.

The observed dynamics of virus are the net effect of both viral replication (caused by the infection of new $CD4^+$ T cells) and viral decay (caused by the natural death of infected cells, or $CD8^+$ T cell killing of infected cells). In the absence of WT-specific $CD8^+$ T cell effects (i.e., in animals lacking the correct MHC), the WT virus has a faster growth rate, because of the fitness cost of the escape mutation (22). This replicative advantage of WT virus scales with the number of remaining $CD4^+$ T cells available to be infected (28). Thus, if $CD8^+$ T cell effects are mediated through cytolysis of infected cells, then the maximum escape rate will be seen when $CD4^+$ T cells are at their minimum (32) and the effects of WT replicative advantage are minimized. This is easily explained by analysis of the model, because the rate of escape is (Equation 6 in the model description in *Materials and Methods*):

$$E(t) = \delta_W - \delta_M - (r_W - r_M)T.$$

If immune response is cytolytic, it has no impact on the replicative capacity of WT virus, which is greater than EM (WT being the fitter strain, $r_W > r_M$), so that escape is maximum when $CD4^+$ T cells are low. This happens when $CD4^+$ T cells are at the minimum, which should also coincide with the peak rate of decay in total virus. At the time of the greatest escape rate, WT should decay much faster than EM (Fig. 3*A*).

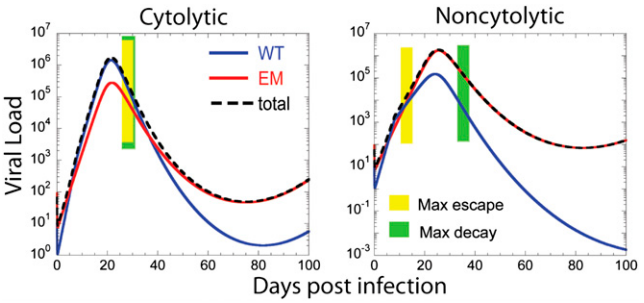

FIGURE 3. Modeling the effects of cytolytic and noncytolytic activity of cytotoxic T cells. The viral load of wild type (WT; blue) and escape mutant (EM; red) viruses are shown over time. Yellow rectangles indicate the maximum escape rate; green rectangles are at the maximum decay rate of total viral load. If the immune response is purely cytolytic, we expect the maximum escape in the acute phase to happen during the decay of virus after the peak, when the decay rate of EM is slower than the decay rate of WT (*left*). If it is purely noncytolytic, the fastest escape would occur during viral growth, and the decay rates of WT and EM after the peak would be similar.

If $CD8^+$ T cell control of virus is mediated through reducing infection of new cells, or reducing viral production from currently infected cells, then the maximum escape rate is seen when viral growth rate is maximum; that is, many $CD4^+$ T cells are available to be infected. Again, this can be understood from the model. In the case of purely noncytolytic control, death rates of WT and EM would not differ much ($\delta_W \approx \delta_M$), but the replicative capacity of WT would become lower than that of EM ($r_W < r_M$), so that

$$E(t) = (r_M - r_W)T.$$

In addition, noncytolytic control would not have much impact on the decay rates of WT and EM after the peak (Fig. 3*B*).

To compare the predictions of the models with experimental data, we plotted the maximum escape rate for each animal against the total viral growth at the time of maximum escape (Fig. 4*A*) or the $CD4^+$ T cell number at the time of maximum escape (Fig. 4*B*). In agreement with the predictions of the noncytolytic model, maximum escape rate was greater when it occurred during growth of viral load than when it occurred during decay (Fig. 4*A*), and was slower when the $CD4^+$ T cell number was lower (Fig. 4*B*). Another possible explanation of the fastest observed escape rate would be that it simply coincides with the highest WT-specific $CD8^+$ T cell count. To test this hypothesis, in Fig. 4*C*, we plot the percentage of the maximum $CD8^+$ T cell number, observed during the period of the maximum escape rate. Figure 4*C* shows that the maximum escape rate occurs at the maximum CD8 number in only two animals. Furthermore, the percentage of maximum CD8 level observed during fastest escape does not correlate with the maximum escape rate (p = 0.2366, Spearman correlation). This indicates that the variations in timing and magnitude of escape rate cannot be explained solely by variations in $CD8^+$ T cell response.

Our model of viral escape at a single epitope describes escape rate as a balance between EM selection advantage because of WT-specific antiviral effect of $CD8^+$ T cells and the fitness cost of escape mutation (28). This picture predicts that, in the case of cytolytic control by $CD8^+$ T cells, increased killing of WT-infected cells should lead to the maximum escape rate during maximum decay of total viral load. The analysis of maximum escape rate in 11 animals revealed this pattern in only two animals (6349, 5614). In contrast, we found that in around half of the animals the fastest escape is during viral load growth, a trend in the escape dynamics completely inconsistent with preferential

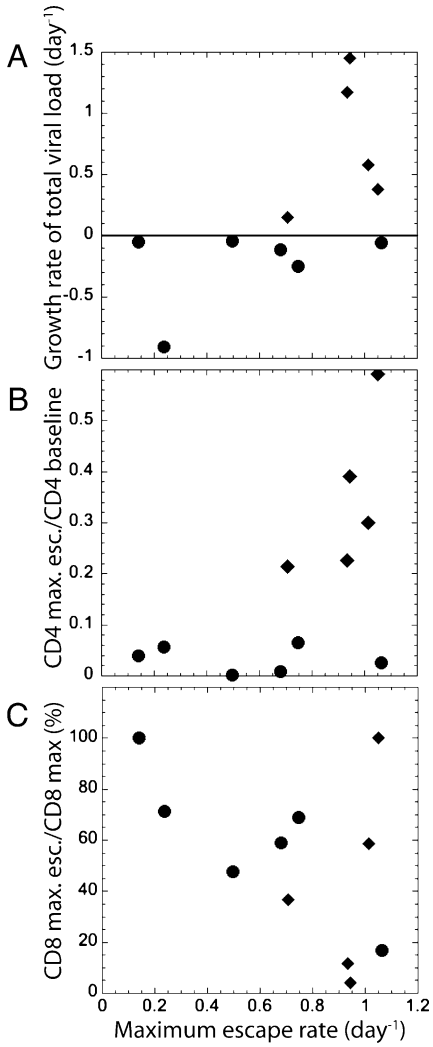

FIGURE 4. High escape rates occur during viral load growth and at high $CD4^+$ T cell numbers. Circles represent the maximum escape rates occurring during viral load decay, and diamonds represent the maximum escape rates during viral decay. *A*, Maximum escape occurs during periods of viral growth or relatively stable viral loads. Only in one animal does the maximum escape occur during a period of high viral decay. *B*, Maximum escape rate occurs at high $CD4^+$ T cell numbers, and animals with low $CD4^+$ T cells at the time of escape show slow escape. Proportion of baseline $CD4^+$ T cells remaining during maximum escape rate is shown. *C*, Maximum escape rate does not generally occur at the highest number of KP9-specific $CD4^+$ T cells. Percentage of the maximum recorded wild type–specific $CD8^+$ T cell number that is observed at the maximum escape rate is shown. Maximum escape rate occurs at the maximum CD8 number in only two animals, showing that the variations in escape rate cannot be explained solely by variations in CD8 response.

cytolysis of WT-infected cells, but in agreement with noncytolytic viral control. However, the number of animals was not sufficient to obtain statistical significance just from analysis of maximum escape rate. This prompted us to investigate the relation between escape dynamics and $CD8^+$ and $CD4^+$ T cell levels at all available time intervals in all animals.

Because the $CD8^+$ T cell activity is the cause of escape, we expected to see positive correlation between escape rate and the number of KP9-specific $CD8^+$ T cells irrespective of whether the mechanism of viral control is cytolytic or noncytolytic. We measured the frequency of KP9-specific $CD8^+$ T cells using MHC class I tetramers, and combined the data on the magnitude of KP9-specific responses and the rate of immune escape (over the subsequent time interval) for all animals over the first 8 wk of infection (Fig. 5*A*). As would be predicted by either cytolytic or noncytolytic mechanisms, we found that the escape rate was significantly correlated with $CD8^+$ T cell number. However, the fact that the fastest escape almost never coincides with the highest CD8 number suggests that escape rate is also strongly modulated by environmental effects such as $CD4^+$ T cell availability (28, 32).

One way to differentiate between cytolytic or noncytolytic control is to determine whether the $CD8^+$ T cell antiviral effect is correlated with the $CD4^+$ T cell number. If the mechanism of viral control is increased killing of WT-infected cells, then WT antiviral effect exerts its impact as a difference in WT and EM death rates. This difference would correlate to the KP9-specific $CD8^+$, but would be independent of target (i.e., $CD4^+$ T) cell frequency. However, if the main mechanism is noncytolytic, resulting in reduced WT replicative capacity, WT-specific antiviral effect would positively correlate with target cell numbers in addition to $CD8^+$ T cell numbers. Positive correlation between WT-specific antiviral effect and target cell numbers is only possible for noncytolytic mechanism of virus control. The expected outcomes for the two types of CD8 response are summarized in Fig. 6.

Next, we found the correlation between WT-specific antiviral effect and $CD4^+$ T cell number (Fig. 5*B*). In a previous study (28) of reversion at KP9 epitope, we found the difference in replicative capacities of KP9 WT and EM in the absence of WT-specific CTL response. We used this result to evaluate the WT-specific antiviral effect as described in *Materials and Methods* (Equation 7). The WT-specific antiviral effect compares the difference in EM and WT growth rates in the presence and absence of KP9-specific $CD8^+$ T cell response, and thus measures the specific immune pressure exerted against the KP9 epitope. According to our model (Equation 7), it should not correlate with $CD4^+$ T cell number if the response is cytolytic, and should correlate positively if the response is noncytolytic. Consistent with noncytolytic mechanism of virus control, WT-specific $CD8^+$ T cell antiviral effect was significantly positively correlated with $CD4^+$ T cell number ($p = 0.0093$, Spearman correlation).

Discussion

The $CD8^+$ T cell response to HIV is crucial for immune control of the virus, and it has usually been assumed that these $CD8^+$ CTLs control virus by direct cytolysis of HIV-infected cells. However, recent studies in SIV-infected macaques have suggested that $CD8^+$ T cells do not alter the life span of productively infected cells in vivo, and thus control of virus in SIV infection may be driven by noncytolytic mechanisms (13, 14). These studies are complicated by the need to deplete $CD8^+$ T cells using Abs, and the consequent perturbation of the host environment. In this study, we analyzed the dynamics of competition between two viral quasispecies differing in their recognition of one immunodominant epitope by $CD8^+$ T cells, in the absence of any perturbation to the host.

We found several aspects of the dynamics of viral competition and immune escape inconsistent with selective $CD8^+$ T cell cytolysis of WT-infected cells: First, if escape were driven exclusively by increased cytolysis of WT-infected cells, then we would expect to see the decay of WT virus being equivalent to the death rate of EM cells plus the escape rate. Instead, the maximum decay rates of WT and EM viruses were similar, and the maximum difference in WT and EM decay rates was much lower than the fastest escape rate. This is consistent with a noncytolytic model of CD8 T cell control, where the death rate of infected cells is determined by viral cytopathic effect or non-CD8 immune recognition, and is constant for both EM and WT viruses.

Our modeling analysis predicts that maximum escape should occur during the decline of viral load if the main control mechanism is cytolytic, and during viral growth if the main mechanism is

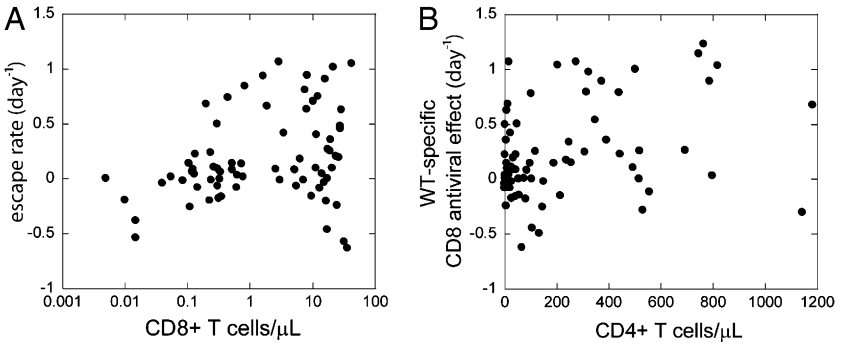

FIGURE 5. Dependence of immune response on wild type (WT)–specific $CD8^+$ T cell and $CD4^+$ T cell numbers. The rate of immune escape or level of $CD8^+$ antiviral effect is plotted for each time period for every animal. *A*, Escape rate is positively correlated with the average KP9-specific $CD8^+$ T cell number for all animals ($p = 0.0152$, Spearman correlation). *B*, There is a significant correlation between WT-specific antiviral effect and $CD4^+$ T cell availability ($p = 0.0093$, Spearman correlation).

noncytolytic. Consistent with a noncytolytic mechanism, the fastest escape rate was often during viral growth instead of during decay, and occurred at high instead of low $CD4^+$ T cell numbers. The model also predicts that the WT antiviral effect (i.e., the suppression of WT in the presence of specific cellular response) should not correlate with CD4 T cell number if control is

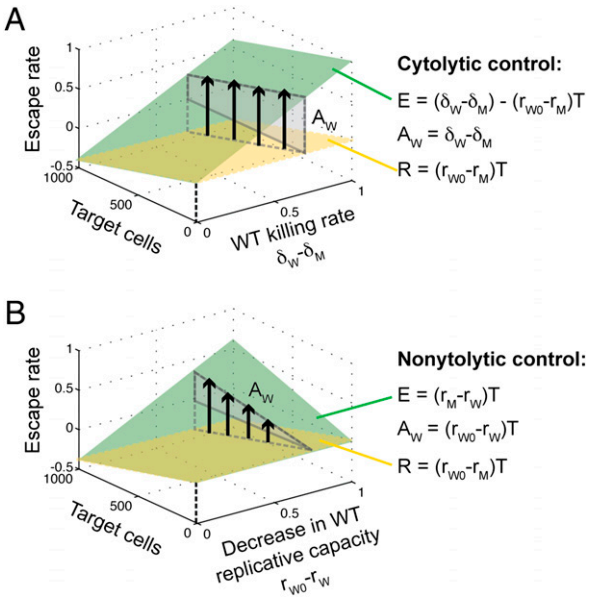

FIGURE 6. Escape rate depending on wild type (WT)–specific antiviral effect and target cell availability in (*A*) cytolytic and (*B*) noncytolytic immune response. Without any WT-specific immune response, WT has higher replicative capacity than escape mutant (EM) because of the fitness costs of escape. Thus, in the absence of an immune response, we see reversion to WT at a rate proportional to the target cell availability (28) (negative escape rate *R* shown as yellow planes). For selection of EM to be possible, the immune response has to be strong enough to overcome the fitness cost of escape mutation (green areas). In the case of a cytolytic immune response against WT virus, this is achieved by increased killing of WT-infected cells (*A*). The effect of WT-specific killing (the WT-specific antiviral effect A_W shown as black arrows) is to shift the difference in growth rates of EM and WT in positive direction by the same amount—independent of target cell levels (green area in *A*). This shift does not change the negative trend of escape rate with target cell number, so that for constant level of immune response, we expect the highest escape rate when target cells are at their lowest point. In the case of noncytolytic control, the immune response reduces the replicative capacity of WT virus (*B*). The effect of this reduction A_W (black arrows in *B*) is to decrease the growth rate of WT by the amount proportional to target cell number. For a constant level of immune response, we would expect the highest escape rate when target cells are the highest. In both cases, escape rate should correlate positively with the level of WT-specific $CD8^+$ T cell response. However, only in the case of noncytolytic control is escape rate positively correlated with the level of the $CD4^+$ T cells.

cytolytic, and should correlate positively if control is noncytolytic. In agreement with the noncytolytic predictions, the WT-specific antiviral effect was positively correlated to the CD4 levels.

The most likely mechanisms of noncytolytic control of virus involve release of soluble factors such as cytokines or chemokines by $CD8^+$ T cells after recognition of their cognate epitope. The important role of soluble factors in virus control has been extensively studied in the past in the search for the "cell antiviral factor" (CAF) (33). These soluble factors were often thought to be secreted into the environment and acting nonspecifically against all neighboring infected cells. In fact, the very existence of immune escape has often been regarded as a proof of the importance of $CD8^+$ T cell killing in the control of HIV/SIV infection. However, the selective control of WT virus that drives immune escape suggests that noncytolytic effects are highly specific to the WT-infected cells. This is consistent with in vitro demonstrations that the secretion of soluble factors is MHC restricted (34). It is therefore possible that such noncytolytic effects are specifically directed to the infected cell that is recognized through TCR-peptide MHC interactions. An alternative explanation is that soluble factors act locally, but that WT and EM infection are compartmentalized, so that WT-infected cells tend to be geographically isolated from EM-infected cells (either as single cells or in clusters) (35). In the presence of compartmentalized infection, WT-infected cells could be selectively inhibited by nonspecific secretion of cytokines into the neighborhood of WT-infected cells. An alternative mechanism to the secretion of soluble factors is that $CD8^+$ T cells do mediate their effects via cytolysis of infected cells, but that this occurs in a "window period" between infection and the production of virus (18). The possibility of such a mechanism is supported by studies showing that Gag-specific $CD8^+$ T cells can recognize SIV-infected cells in vitro within hours of exposure to virus (36). Because in our studies the assay measures only the decay of virus made by productively infected cells and not cells that are killed before release of any virions, our analysis is unable to discriminate between noncytolytic control and killing of infected cells in this window period before viral production.

Understanding the mechanisms of immune control of HIV is important to both pathogenesis and vaccine development. Our studies of the dynamics of immune escape in vivo in $SHIV_{mn229}$ infection support the existence of a noncytolytic $CD8^+$ T cell-mediated, MHC class I–restricted mechanism of immune control that is highly specific for the cognate epitopes recognized by virus-specific $CD8^+$ T cells. In this way, $CD8^+$ T cells can drive the rapid selection of EM virus during acute infection in the absence of direct killing of infected cells. The importance of our study is the simultaneous measurement of viral dynamics in two viral strains with differential CD8 T cell recognition, but present in the same host environment and in the absence of immune manipulation. The rate of escape demonstrates the strength of

CD8 T cell control in this system, and our goal was to differentiate the mechanisms of this control. Despite the benefits of this system, it also has a number of limitations. First, this is not HIV, but rather a CXCR4 tropic SHIV infection, and thus does not prove the same mechanisms act in HIV. Clearly, a study of escape dynamics in closely sampled early HIV infection would be required to directly demonstrate this effect in human infection. However, despite the differences, infected cell dynamics and immune control appear quite similar between SHIV, SIV, and HIV. There are similar death rates of infected cells, as determined from the decay rate of virus during antiretroviral therapy (37–39). Escape rates in CXCR4 tropic $SHIV_{mn229}$ and CCR5 tropic SIV are of similar magnitudes when compared in the same phases of infection (23). This suggests that similar mechanisms control virus in these infections, despite the differences in the subsets of susceptible T cells. It remains possible, however, that the mechanisms of immune control differ in HIV, or that cytolytic mechanisms play a more crucial role in "elite controller" individuals or macaques, or both.

Another limitation of our study is the frequency of sampling, which may limit our ability to measure viral kinetics if they vary rapidly over short intervals. However, the samples were at 3- to 7-d intervals out to day 28, which is more frequent than the usual sampling period in HIV. Moreover, the extreme sensitivity of the QRT-PCR assay to detect low levels of virus gives us a large dynamic range over which viral kinetics can be compared. Thus, it seems unlikely that sampling frequency has biased out results. Finally, we have measured the kinetics of two viral strains differing at the KP9 epitope, but have not explicitly considered recognition by CD8 T cells at other epitopes, or infected cell killing by other mechanisms such as NK cells or viral cytopathic effect. We expect these nonepitope-specific factors to act equally on WT and EM viruses; thus, the death rate of EM-infected cells should reflect the sum of these "background" killing rates. The rapid escape rate indicates that WT virus is under some additional pressure, which in the case of cytolysis should be an additional killing by KP9-specific cells, on top of this background death rate. The fact that the death rate of WT and EM cells is not significantly different suggests these other factors do indeed act similarly on both strains of virus.

The results of this study and the recent CD8 depletion studies (13, 14) suggest that analyses of $CD8^+$ T cell control of HIV during natural infection and by vaccination should focus more closely on the noncytolytic function of CD8 T cells. This is consistent with studies now suggesting that CD8 T cells capable of liberating multiple cytokines/chemokines (so-called polyfunctional T cells) are more efficient at controlling HIV infection (40–42). Defining more carefully the particular molecules and mechanisms most responsible for noncytolytic control of HIV could lead to the more rational design of better T cell–based HIV vaccines.

Acknowledgments

We thank Ruy M. Ribeiro and Alan S. Perelson for careful reading of the manuscript and useful suggestions.

Disclosures

The authors have no financial conflicts of interest.

References

1. Borrow, P., H. Lewicki, B. H. Hahn, G. M. Shaw, and M. B. Oldstone. 1994. Virus-specific CD8+ cytotoxic T-lymphocyte activity associated with control of viremia in primary human immunodeficiency virus type 1 infection. *J. Virol.* 68: 6103–6110.
2. Jin, X., D. E. Bauer, S. E. Tuttleton, S. Lewin, A. Gettie, J. Blanchard, C. E. Irwin, J. T. Safrit, J. Mittler, L. Weinberger, et al. 1999. Dramatic rise in plasma viremia after CD8(+) T cell depletion in simian immunodeficiency virus-infected macaques. *J. Exp. Med.* 189: 991–998.
3. Koup, R. A., J. T. Safrit, Y. Cao, C. A. Andrews, G. McLeod, W. Borkowsky, C. Farthing, and D. D. Ho. 1994. Temporal association of cellular immune responses with the initial control of viremia in primary human immunodeficiency virus type 1 syndrome. *J. Virol.* 68: 4650–4655.
4. Borrow, P., H. Lewicki, X. Wei, M. S. Horwitz, N. Peffer, H. Meyers, J. A. Nelson, J. E. Gairin, B. H. Hahn, M. B. Oldstone, and G. M. Shaw. 1997. Antiviral pressure exerted by HIV-1-specific cytotoxic T lymphocytes (CTLs) during primary infection demonstrated by rapid selection of CTL escape virus. *Nat. Med.* 3: 205–211.
5. Goulder, P. J., and D. I. Watkins. 2004. HIV and SIV CTL escape: implications for vaccine design. *Nat. Rev. Immunol.* 4: 630–640.
6. Leslie, A. J., K. J. Pfafferott, P. Chetty, R. Draenert, M. M. Addo, M. Feeney, Y. Tang, E. C. Holmes, T. Allen, J. G. Prado, et al. 2004. HIV evolution: CTL escape mutation and reversion after transmission. *Nat. Med.* 10: 282–289.
7. Brumme, Z. L., and P. R. Harrigan. 2006. The impact of human genetic variation on HIV disease in the era of HAART. *AIDS Rev.* 8: 78–87.
8. Kaslow, R. A., M. Carrington, R. Apple, L. Park, A. Muñoz, A. J. Saah, J. J. Goedert, C. Winkler, S. J. O'Brien, C. Rinaldo, et al. 1996. Influence of combinations of human major histocompatibility complex genes on the course of HIV-1 infection. *Nat. Med.* 2: 405–411.
9. Scherer, A., J. Frater, A. Oxenius, J. Agudelo, D. A. Price, H. F. Günthard, M. Barnardo, L. Perrin, B. Hirschel, R. E. Phillips, A. R. McLean; Swiss HIV Cohort Study. 2004. Quantifiable cytotoxic T lymphocyte responses and HLA-related risk of progression to AIDS. *Proc. Natl. Acad. Sci. USA* 101: 12266–12270.
10. Migueles, S. A., C. M. Osborne, C. Royce, A. A. Compton, R. P. Joshi, K. A. Weeks, J. E. Rood, A. M. Berkley, J. B. Sacha, N. A. Cogliano-Shutta, et al. 2008. Lytic granule loading of CD8+ T cells is required for HIV-infected cell elimination associated with immune control. *Immunity* 29: 1009–1021.
11. Nixon, D. F., A. R. Townsend, J. G. Elvin, C. R. Rizza, J. Gallwey, and A. J. McMichael. 1988. HIV-1 gag-specific cytotoxic T lymphocytes defined with recombinant vaccinia virus and synthetic peptides. *Nature* 336: 484–487.
12. Chea, S., C. J. Dale, R. De Rose, I. A. Ramshaw, and S. J. Kent. 2005. Enhanced cellular immunity in macaques following a novel peptide immunotherapy. *J. Virol.* 79: 3748–3757.
13. Klatt, N. R., E. Shudo, A. M. Ortiz, J. C. Engram, M. Paiardini, B. Lawson, M. D. Miller, J. Else, I. Pandrea, J. D. Estes, et al. 2010. CD8+ lymphocytes control viral replication in SIVmac239-infected rhesus macaques without decreasing the lifespan of productively infected cells. *PLoS Pathog.* 6: e1000747.
14. Wong, J. K., M. C. Strain, R. Porrata, E. Reay, S. Sankaran-Walters, C. C. Ignacio, T. Russell, S. K. Pillai, D. J. Looney, and S. Dandekar. 2010. In vivo CD8+ T-cell suppression of siv viremia is not mediated by CTL clearance of productively infected cells. *PLoS Pathog.* 6: e1000748.
15. Okoye, A., H. Park, M. Rohankhedkar, L. Coyne-Johnson, R. Lum, J. M. Walker, S. L. Planer, A. W. Legasse, A. W. Sylwester, M. Piatak, Jr., et al. 2009. Profound CD4+/CCR5+ T cell expansion is induced by CD8+ lymphocyte depletion but does not account for accelerated SIV pathogenesis. *J. Exp. Med.* 206: 1575–1588.
16. Barouch, D. H., S. Santra, J. E. Schmitz, M. J. Kuroda, T. M. Fu, W. Wagner, M. Bilska, A. Craiu, X. X. Zheng, G. R. Krivulka, et al. 2000. Control of viremia and prevention of clinical AIDS in rhesus monkeys by cytokine-augmented DNA vaccination. *Science* 290: 486–492.
17. Shiver, J. W., T. M. Fu, L. Chen, D. R. Casimiro, M. E. Davies, R. K. Evans, Z. Q. Zhang, A. J. Simon, W. L. Trigona, S. A. Dubey, et al. 2002. Replication-incompetent adenoviral vaccine vector elicits effective anti-immunodeficiency-virus immunity. *Nature* 415: 331–335.
18. Davenport, M. P., R. M. Ribeiro, L. Zhang, D. P. Wilson, and A. S. Perelson. 2007. Understanding the mechanisms and limitations of immune control of HIV. *Immunol. Rev.* 216: 164–175.
19. Davenport, M. P., R. M. Ribeiro, and A. S. Perelson. 2004. Kinetics of virus-specific CD8+ T cells and the control of human immunodeficiency virus infection. *J. Virol.* 78: 10096–10103.
20. Davenport, M. P., L. Zhang, A. Bagchi, A. Fridman, T. M. Fu, W. Schleif, J. W. Shiver, R. M. Ribeiro, and A. S. Perelson. 2005. High-potency human immunodeficiency virus vaccination leads to delayed and reduced CD8+ T-cell expansion but improved virus control. *J. Virol.* 79: 10059–10062.
21. De Rose, R., C. J. Batten, M. Z. Smith, C. S. Fernandez, V. Peut, S. Thomson, I. A. Ramshaw, B. E. Coupar, D. B. Boyle, V. Venturi, et al. 2007. Comparative efficacy of subtype AE simian-human immunodeficiency virus priming and boosting vaccines in pigtail macaques. *J. Virol.* 81: 292–300.
22. Fernandez, C. S., I. Stratov, R. De Rose, K. Walsh, C. J. Dale, M. Z. Smith, M. B. Agy, S. L. Hu, K. Krebs, D. I. Watkins, et al. 2005. Rapid viral escape at an immunodominant simian-human immunodeficiency virus cytotoxic T-lymphocyte epitope exacts a dramatic fitness cost. *J. Virol.* 79: 5721–5731.
23. Loh, L., J. Petravic, C. J. Batten, M. P. Davenport, and S. J. Kent. 2008. Vaccination and timing influence SIV immune escape viral dynamics in vivo. *PLoS Pathog.* 4: e12.
24. Asquith, B., C. T. Edwards, M. Lipsitch, and A. R. McLean. 2006. Inefficient cytotoxic T lymphocyte-mediated killing of HIV-1-infected cells in vivo. *PLoS Biol.* 4: e90.
25. Ganusov, V. V., and R. J. De Boer. 2006. Estimating costs and benefits of CTL escape mutations in SIV/HIV Infection. *PLOS Comput. Biol.* 2: e24.
26. Fernandez, C. S., M. Z. Smith, C. J. Batten, R. De Rose, J. C. Reece, E. Rollman, V. Venturi, M. P. Davenport, and S. J. Kent. 2007. Vaccine-induced T cells control reversion of AIDS virus immune escape mutants. *J. Virol.* 81: 4137–4144.

27. Batten, C. J., R. De Rose, K. M. Wilson, M. B. Agy, S. Chea, I. Stratov, D. C. Montefiori, and S. J. Kent. 2006. Comparative evaluation of simian, simian-human, and human immunodeficiency virus infections in the pigtail macaque (*Macaca nemestrina*) model. *AIDS Res. Hum. Retroviruses* 22: 580–588.
28. Petravic, J., L. Loh, S. J. Kent, and M. P. Davenport. 2008. CD4+ target cell availability determines the dynamics of immune escape and reversion in vivo. *J. Virol.* 82: 4091–4101.
29. Lloyd, A. L. 2001. The dependence of viral parameter estimates on the assumed viral life cycle: limitations of studies of viral load data. *Proc. Biol. Sci.* 268: 847–854.
30. Nowak, M. A., and R. M. May. 2000. *Virus dynamics: mathematical principles of immunology and virology.* Oxford University Press, Oxford, United Kingdom.
31. Nowak, M. A., A. L. Lloyd, G. M. Vasquez, T. A. Wiltrout, L. M. Wahl, N. Bischofberger, J. Williams, A. Kinter, A. S. Fauci, V. M. Hirsch, and J. D. Lifson. 1997. Viral dynamics of primary viremia and antiretroviral therapy in simian immunodeficiency virus infection. *J. Virol.* 71: 7518–7525.
32. Davenport, M. P., L. Loh, J. Petravic, and S. J. Kent. 2008. Rates of HIV immune escape and reversion: implications for vaccination. *Trends Microbiol.* 16: 561–566.
33. Levy, J. A. 2003. The search for the CD8+ cell anti-HIV factor (CAF). *Trends Immunol.* 24: 628–632.
34. Yang, O. O., S. A. Kalams, A. Trocha, H. Cao, A. Luster, R. P. Johnson, and B. D. Walker. 1997. Suppression of human immunodeficiency virus type 1 replication by CD8+ cells: evidence for HLA class I-restricted triggering of cytolytic and noncytolytic mechanisms. *J. Virol.* 71: 3120–3128.
35. Cheynier, R., S. Henrichwark, F. Hadida, E. Pelletier, E. Oksenhendler, B. Autran, and S. Wain-Hobson. 1994. HIV and T cell expansion in splenic white pulps is accompanied by infiltration of HIV-specific cytotoxic T lymphocytes. *Cell* 78: 373–387.
36. Sacha, J. B., C. Chung, E. G. Rakasz, S. P. Spencer, A. K. Jonas, A. T. Bean, W. Lee, B. J. Burwitz, J. J. Stephany, J. T. Loffredo, et al. 2007. Gag-specific CD8+ T lymphocytes recognize infected cells before AIDS-virus integration and viral protein expression. *J. Immunol.* 178: 2746–2754.
37. Chen, H. Y., M. Di Mascio, A. S. Perelson, D. D. Ho, and L. Zhang. 2007. Determination of virus burst size in vivo using a single-cycle SIV in rhesus macaques. *Proc. Natl. Acad. Sci. USA* 104: 19079–19084.
38. Davenport, M. P., L. Zhang, J. W. Shiver, D. R. Casmiro, R. M. Ribeiro, and A. S. Perelson. 2006. Influence of peak viral load on the extent of CD4+ T-cell depletion in simian HIV infection. *J. Acquir. Immune Defic. Syndr.* 41: 259–265.
39. Ramratnam, B., S. Bonhoeffer, J. Binley, A. Hurley, L. Zhang, J. E. Mittler, M. Markowitz, J. P. Moore, A. S. Perelson, and D. D. Ho. 1999. Rapid production and clearance of HIV-1 and hepatitis C virus assessed by large volume plasma apheresis. *Lancet* 354: 1782–1785.
40. Betts, M. R., M. C. Nason, S. M. West, S. C. De Rosa, S. A. Migueles, J. Abraham, M. M. Lederman, J. M. Benito, P. A. Goepfert, M. Connors, et al. 2006. HIV nonprogressors preferentially maintain highly functional HIV-specific CD8+ T cells. *Blood* 107: 4781–4789.
41. Daucher, M., D. A. Price, J. M. Brenchley, L. Lamoreaux, J. A. Metcalf, C. Rehm, E. Nies-Kraske, E. Urban, C. Yoder, D. Rock, et al. 2008. Virological outcome after structured interruption of antiretroviral therapy for human immunodeficiency virus infection is associated with the functional profile of virus-specific CD8+ T cells. *J. Virol.* 82: 4102–4114.
42. Pantaleo, G., and R. A. Koup. 2004. Correlates of immune protection in HIV-1 infection: what we know, what we don't know, what we should know. *Nat. Med.* 10: 806–810.